View metadata, citation and similar papers at core.ac.uk
brought to you by CORE
provided by Woods Hole Open Access Server

Strontium isotopes in Chilean rivers: the flux of unradiogenic continental Sr to seawater.

Katherina Fiege [a,b], Christian A. Miller [a,c], Laura F. Robinson [a], Ricardo Figueroa [d], Bernhard Peucker-Ehrenbrink [a,e*]

[a] *Department of Marine Chemistry and Geochemistry, Woods Hole Oceanographic Institution, Woods Hole, MA 02543, USA;* [b] *Institute of Geology and Paleontology, University of Heidelberg, 69120 Heidelberg, Germany;* [c] *MIT/WHOI Joint Program in Oceanography, USA;* [d] *Aquatic Systems Research Unit, Environmental Science Center EULA-Chile, University of Concepcion, PO Box 160-C, Concepcion, Chile;* [e] *Laboratoire d'Etudes en Géophysique et Océanographie Spatiale (LEGOS), CNES/ENRS/UPS/IRD, Observatoire Midi-Pyrénées, 14 av. E. Belin, 31400 Toulouse, France.*

* *Corresponding author: behrenbrink@whoi.edu, phone: 01 508 289 2518, fax: 01 508 457 2193.*

Abstract: 214 words, Text: 3624 words, 3 Figures, 1 Table.

last saved: 08/26/2009 (12:00)

Keywords: strontium, river, seawater, Chile, Andes, weathering.

Abstract

Analyses of Chilean river waters indicate that the average yield of unradiogenic Sr (~517 moles Sr km^{-2} yr^{-1}, $^{87}Sr/^{86}Sr$ ~0.7057) from western South America (1,220,853 km^2) into the southeastern Pacific Ocean is ~2-4 times higher than that from Iceland (~110 moles Sr km^{-2} yr^{-1},

21 $^{87}Sr/^{86}Sr$ ~0.7025) and the Deccan traps, but lower than fluxes of unradiogenic Sr from ocean
22 islands in the Lesser Antilles and Réunion. The Sr flux from western South America accounts
23 for about 1.8% of the annual dissolved Sr delivered to the ocean via rivers. If Chilean rivers
24 analyzed in this study accurately characterize runoff from western South America, active
25 convergent continental margins release about as much unradiogenic Sr to seawater as a 0-1 Myr
26 old mid-ocean ridge segment of equivalent length. Modulations of the flux of unradiogenic Sr
27 from active margins over geologic time scales have to be considered as an additional driving
28 force of change in the marine Sr isotope record, supplementing temporal variations in the
29 submarine hydrothermal flux as a source of unradiogenic Sr to seawater. Such modulations can
30 be driven by changes in the surface exposure of volcanic arc terrains, changes in climate, ocean
31 currents and geographic latitude due to plate tectonics, as well as topographic changes that can
32 affect local rainfall, runoff and erosion.

33

34 **1. Introduction**

35 Of the radiogenic isotope systems, the $^{87}Sr/^{86}Sr$ of continental runoff has been studied most
36 comprehensively (e.g., Faure et al., 1967; Fisher and Stueber, 1976; Wadleight et al., 1985;
37 Åberg and Wickman, 1987; Goldstein and Jacobsen, 1987; Palmer and Edmond, 1989, 1992;
38 Cameron and Hattori, 1997). Prior to the discovery of submarine hydrothermal vents in 1977 the
39 marine Sr isotope record was viewed as reflecting the changing balance between two contrasting
40 continental sources; unradiogenic runoff from unradiogenic basaltic terrains and radiogenic Sr
41 derived from granitic terrains (Brass, 1976). Since the discovery of submarine hydrothermal
42 vents the marine strontium isotope record has generally been interpreted and modeled as a

43 mixture of unradiogenic hydrothermal Sr and radiogenic continental Sr with minor contributions
44 from the diagenesis of marine sediments (e.g., Albarede et al., 1981; Palmer and Edmond, 1989).

45 To date, ~193 exorheic rivers representing ~47% of the total continental runoff have been
46 characterized at least once for $^{87}Sr/^{86}Sr$ and Sr concentration (Peucker-Ehrenbrink, in prep., and
47 references therein). Despite this significant body of work, runoff from several large-scale
48 drainage regions remains poorly defined and, thus far, has had to be approximated through
49 comparison of similarities in bedrock characteristics with better-characterized drainage areas
50 (Palmer and Edmond, 1989).

51 Of all large continental drainage regions (Graham et al., 1999, 2000; Peucker-Ehrenbrink,
52 2009), the region of South America (1,220,853 km^2) that drains into the southeastern Pacific is
53 characterized by the youngest bedrock (~96 Myr) and the highest percentage (37.3%) of exposed
54 extrusive bedrock (Peucker-Ehrenbrink and Miller, 2007). On average, this region also receives
55 abundant rainfall (e.g., New et al., 2002; Muñoz et al., 2007) and generates about 4% of the
56 annual global runoff from the equivalent of 1% of the total continental land area. Surprisingly,
57 we could not find any published Sr isotope analysis of waters draining this region, only a
58 $^{87}Sr/^{86}Sr$ value of 0.7075 for hydrous precipitates in Atacama Desert soils (Rech et al., 2003).
59 Even the comprehensive review of Palmer and Edmond (1989) did not attempt to include this
60 drainage region into the assessment of the continental flux of Sr into the oceans, although they
61 did predict that inclusion of runoff from "relatively young volcanic island arc terrains of the
62 western Pacific, Cenozoic platform carbonates and plateau basalts" (Palmer and Edmond, 1989,
63 p. 22) would shift the empirically-determined average $^{87}Sr/^{86}Sr$ of continental runoff from 0.7119
64 to 0.7114. This study was conducted to estimate the isotope composition and flux of continental
65 Sr to the southeastern Pacific Ocean.

66

67 **2. Regional Geology**

68 Rivers investigated in this study were sampled in central and southern Chile and are part of a
69 larger number of mid-size river basins that drain the western side of South America into the
70 southwestern Pacific. As the regional geology and tectonic setting of the western Andes as well
71 as the geological makeup of Chilean drainage basins have recently been summarized (Stern,
72 2004; Muñoz et al., 2007) we restrict the discussion of these features to a brief summary. The
73 basins investigated by us are dominated by Pleistocene and Holocene sedimentary sequences,
74 which commonly consist of fluvial, alluvial or deltaic deposits. Volcanic sequences are often
75 intercalated with sedimentary units and are mainly composed of volcanic ash, pyroclastics and
76 basaltic to dacitic lavas. These units vary in age from Jurassic to Quaternary. Intrusive and
77 metamorphic rocks are more abundant in the southern river basins. The intrusive rocks include
78 diorites, granites, tonalites, and gabbros, whereas amphibolites, phengites, metapelites,
79 metacherts and rare ultramafic rocks dominate metamorphic sequences of Paleozoic to Triassic
80 age. The locations of the river water samples collected in this area are shown in Figure 1 and are
81 listed in Table 1.

82 The lithologic composition and age structure of large-scale continental drainage regions
83 (Graham et al., 1999, 2000) has been analyzed by Peucker-Ehrenbrink and Miller (2007).
84 Among all drainage regions, the drainage area of western South America stands out as the region
85 with the youngest average bedrock age (96 Myr) and also as the area most dominated by
86 extrusive bedrock (37.3%). The $^{87}Sr/^{86}Sr$ of the basaltic arc rocks from the southern volcanic
87 zone of the Andes ranges from 0.70384 to 0.70451 (Hickey et al., 1986). These values are

88 similar to those of the northern Andean volcanic zone, but less radiogenic than the central
89 Andean volcanic zone.

90 Runoff from Chile into the eastern Pacific Ocean varies strongly with latitude. North of
91 latitude 32.5°S runoff is almost negligible as evaporation dominates the water balance. Muñoz
92 et al. (2007) show that annual runoff increases from less than 100 mm north of 32.5°S to >800
93 mm south of 35°S, and reaches >2000 mm for the BioBio River and other rivers south of 38°S.
94 Rivers analyzed by us were sampled between latitudes 33.5°S and 42.5°S and thus capture the
95 region that generates the majority of the runoff in Chile. Regions in northern Chile and Peru (36
96 km^3 runoff per year from a Peruvian drainage area of 279,689 km^2) generate little runoff into the
97 western Pacific. In contrast, runoff into the eastern Pacific from Colombia (260 km^3 yr^{-1}) and
98 Ecuador (116 km^3 yr^{-1}, with 48% of the total coming from the Esmeralda River system) is
99 volumetrically significant with respect to the total runoff into the Pacific Ocean from the western
100 side of South America (~1266 km^3 yr^{-1}; Peucker-Ehrenbrink, 2009).

101

102 **3. Sampling and analytical methods**

103 All samples were filtered in the field through 0.45 μm Sterivex HV cartridge filters using 60
104 ml all-plastic syringes (Henke-Sass-Wolf GmbH) and stored in precleaned 125 ml PE bottles (EP
105 Scientific). Samples were not acidified, but most were kept refrigerated after they had arrived at
106 WHOI. Some basic sample properties such as temperature, pH, and conductivity were
107 determined in the field on some samples (see Table 1).

108 Samples were analyzed for major anions (Cl and SO_4) by ion chromatography (Dionex).
109 Major and some trace cations (Na, Mg, K, Ca, Rb, Sr, Ba) were determined by single-collector

ICPMS (ThermoFinnigan ELEMENT2). Concentrations of Mg, Ca, Sr and Ba were determined by isotope dilution, whereas Na, K and Rb were quantified using standard calibration curves, prepared from single element standard solutions (NIST 3100 series).

Strontium was quantitatively separated and purified from the samples using Sr-Spec (Eichrom) resin in 300 µl columns. Samples were loaded in 1 ml 3.5N HNO_3 and Sr was eluted with 5 ml deionized water. Recovery was quantitative and separation from potential isobaric interferences Ca and Rb was excellent, as demonstrated by average $^{88}Sr/^{44}Ca$ and $^{88}Sr/^{85}Rb$ values in the eluant of $1x10^4$ and $8x10^4$, respectively. Strontium isotope compositions were determined with a ThermoElectron NEPTUNE multicollector ICPMS. Whenever possible we optimized the ^{88}Sr ion beam intensity to ~45 V (10^{11} Ω resistor). Under these conditions ~200 ng Sr was consumed per analysis. Krypton and Rb interferences were monitored and corrected off-line. The importance of off-line Kr corrections increases depending on the Kr levels detected at the time of analyses. For reasons we do not fully understand, ion beam intensities on masses 82 and 83 vary over weeks and months between less than 1 mV to >10 mV, and were ~8 mV on the day of analysis. Isobaric interferences from ^{86}Kr on ^{86}Sr are corrected by using ^{84}Kr to subtract Kr until the $^{84}Sr/^{88}Sr$ equals the canonical value of 0.00675476 (Hart et al., 2004), while iteratively correcting for mass bias. The fact that the $^{86}Sr/^{84}Sr$ is ~17.7 whereas the $^{86}Kr/^{84}Kr$ is ~0.3 results in large error demagnification when correcting ^{86}Sr for ^{86}Kr contributions with this scheme. Two analyses of the NBS 987 standard reference material that were measured with the river water samples and corrected for Kr and instrumental mass bias using the above scheme yielded $^{87}Sr/^{86}Sr$ values of 0.710295 and 0.710298. Reported $^{87}Sr/^{86}Sr$ values are normalized to a NBS 987 value of 0.710240 (see table 1) and are listed to the 5^{th} decimal place owing to the uncertainties in the Kr correction ($\leq \pm 100$ ppm, 2σ).

4. Results

The analytical data are summarized in Table 1 and the best correlation between concentrations of Sr with any of the major ions, Ca, is shown in Fig 2A. We have also compiled available information on annual runoff (in $km^3\ yr^{-1}$) and drainage basin sizes (in km^2) (Dirección General de Aguas, 1998; Muñoz et al., 2007) in order to extrapolate our findings to the large-scale drainage area of western South America (Graham et al., 1999, 2000). Not all rivers were sampled at their mouths, and some were sampled only along major tributaries (e.g., Calle Calle river in the Valdivia river basin; Tinguiririca river in the Rapel river basin). For instance, the Tinguiririca river (sample 22) was sampled upstream of the confluence with the Cachapoal river (6370 km^2; Gobierno de Chile, 2004) that together form the Rapel river. The Tinguiririca drainage basin (4730 km^2) is the smaller of the two major tributary basins that make up the Rapel drainage basin (13,695 km^2) but we presume that sample 22 is representative of the Rapel river. Despite this deficiency, we presume that the data are representative of the major drainage basins they represent. Where we do have multiple samples from the same river system the $^{87}Sr/^{86}Sr$ values are either rather homogeneous (Tolten river), decrease (Itata river) or increase (BioBio river) slightly towards the coast, and thus provide no evidence for systematic bias of the $^{87}Sr/^{86}Sr$ values.

In the few cases where data on drainage basin size and/or annual water discharge were unavailable (Mapocho, Rio Llonco, Rio Pichicolo, Rio Huinay) we did not include those river basins in our analysis. This does not significantly bias our results because contributions from those rivers are small owing to their small size (e.g., Huinay, Pichicolo, Lonco), or because their isotope composition and Sr concentration are similar to the large rivers we do have data for (e.g.,

Mapocho). The radiogenic ($^{87}Sr/^{86}Sr$=0.70986) Andalien river is a small river draining the Coastal Mountain Range between the Itata river in the North and the BioBio river in the South. In contrast to the BioBio and Itata rivers that drain the Andes and are thus affected by both rainfall and snow melt, runoff in the Andalien river is only determined by rainfall in the Coastal Mountain Range that varies smoothly between 10-50 mm per month during the austral summer and 150-200 mm per month during the austral winter (Muñoz et al., 2007). We use an average runoff of 0.48 $km^3\ yr^{-1}$ that is based on an average of low (austral summer, 0.08 $km^3\ yr^{-1}$) and high (austral winter, 0.9 $km^3\ yr^{-1}$) runoff estimates given in Quiñones and Montes (2001). Our estimate of the drainage basin area of ~850 km^2 is based on a map of the drainage basin outline in Habit et al. (2007). The overall contribution of this radiogenic river to the total flux of Sr is negligible.

5. Discussion

5.1. Average $^{87}Sr/^{86}Sr$ and Sr concentration of Chilean rivers

The average $^{87}Sr/^{86}Sr$, weighted according to Sr concentration (average: 0.496 μM) and average discharge from nine rivers, is 0.7057 (Fig. 2B, star). The weighting procedure does not introduce significant bias because $^{87}Sr/^{86}Sr$ does not correlate with Sr concentration and the non-weighted average (0.70537) and median (0.70458) $^{87}Sr/^{86}Sr$ are similar to the flux-weighted isotope composition (0.7057). This weighted average value does not change significantly if corrections are made for atmospheric, i.e. recycled, Sr of marine origin. If all Cl in the rivers is ultimately derived from seawater with a molar Cl/Sr value of 6260, between 1% and 5% of the Sr in most rivers analyzed could be of seawater origin. Exceptions are the Rio Pichicolo (CH049, highest Sr concentration, Fig. 2B) that receives contributions from hydrothermal

179 springs and two rivers draining into the fjords of southern Chile - the Rio Llonco (CH058) and
180 Rio Huinay (CH059). Based on the Cl concentrations, all of the Sr in the Rio Pichicolo could be
181 of seawater origin, though the isotopic composition of 0.70442 that is similar to values of
182 volcanic rocks in Chile (Hickey et al., 1986; Notsu et al., 1987) demonstrates that this cannot be
183 the case. Based on measured Cl concentrations, as much as one third of the Sr in the Rio Llonco
184 could be derived from seawater. The isotope composition of the Rio Llonco of 0.70908 and the
185 low Sr concentration of 0.016 μM indicates that a significant portion of the riverine Sr could
186 indeed be of marine origin. Correcting for this contribution, however, will not significantly
187 change the Sr isotope composition of the non-marine component. Only 0.25% of the Sr in the
188 Rio Huinay (Fjord district, sample CH059) can be recycled seawater Sr. The isotope
189 composition of 0.70565 indicates that most of the Sr is of non-marine origin, and corrections for
190 marine inputs will not significantly affect this value. In summary, we consider the weighted
191 average $^{87}Sr/^{86}Sr$ of 0.7057 as representative of the continental runoff from Chile into the
192 southeastern Pacific Ocean.

193

194 *5.2. Average* $^{87}Sr/^{86}Sr$ and Sr flux to the southeastern Pacific Ocean.

195 The annual Sr flux from the entire large-scale drainage region of western South America is
196 estimated by extrapolating the results from the Chilean rivers analyzed in this study to the entire
197 large-scale drainage region. The geologic similarities between Peru, Ecuador and Colombia with
198 Chile allow us to assume that the isotope composition of runoff of all the rivers draining into the
199 eastern Pacific is similar to that measured in Chilean rivers. This approach is justified by
200 considering the similarities in $^{87}Sr/^{86}Sr$ between the Northern Volcanic Zone of the Andes
201 (Colombia, Ecuador) and the Southern Volcanic Zone of central and southern Chile (Stern,

2004). The Central Volcanic Zone (southern Peru, northern Chile) is characterized by more radiogenic $^{87}Sr/^{86}Sr$, but low runoff limits its contribution to the dissolved Sr flux into the eastern Pacific Ocean (see review by Stern, 2004). The extrapolated Sr flux for the entire drainage region of western South America is ~6.3×10^8 moles per year, equivalent to ~1.8% of the global riverine Sr flux (3.33×10^{10} moles per year; Palmer and Edmond, 1989). This flux corresponds to an average Sr yield of 517 moles Sr km^{-2} yr^{-1} that we compare in the following section with estimates from three other extensively studied drainage regions dominated by volcanic lithologies: Iceland (Gannoun et al., 2006), the Lesser Antilles and Réunion (Rad et al., 2007), and the Indian Deccan Traps (Dessert et al., 2001).

5.3. Comparison of $^{87}Sr/^{86}Sr$ and Sr flux from the Andean arc with Iceland, the Lesser Antilles and Reunion, and the Deccan Traps.

Based on sampling of Icelandic rivers that account for ~35 km^3 runoff per year, the average Sr concentration in Icelandic rivers is 0.068 μM (6 ng g^{-1}; Gannoun et al., 2006; see Fig. 3, open triangles). This is much less than the runoff-weighted average Sr concentration in Chilean rivers of ~0.5 μM (43 ng g^{-1}). If the dissolved Sr concentration estimated by Gannoun et al. (2006) is typical for Icelandic rivers (170-198 km^3 runoff per year; Baumgartner and Reichel, 1975; Dessert et al., 2003), about 1.2×10^7 moles of dissolved Sr, or 110 moles Sr km^{-2} yr^{-1}, are delivered annually to the ocean by Icelandic rivers. Similarly, if the $^{87}Sr/^{86}Sr$ analysis of the Austari Jökulsa of 0.7025 (Gannoun et al., 2006) is characteristic of Icelandic rivers, runoff from Iceland is isotopically similar to the depleted upper mantle.

Weathering of the Deccan flood basalts delivers approximately 3.8×10^8 mol Sr yr^{-1}, or 705 moles Sr km^{-2} yr^{-1}, equivalent to ~1% of the global riverine flux of Sr to the ocean (Dessert et al.,

2001; Fig. 3, open squares). This flux is derived from an area that accounts for only about 0.5% of the continental land area, indicative of the disproportionate contribution of basalt weathering to continental Sr runoff. Compared to most other large igneous provinces, however, Deccan flood basalts are unusually radiogenic ($^{87}Sr/^{86}Sr$ 0.705-0.715) and thus generate runoff with $^{87}Sr/^{86}Sr$ of 0.7076 to 0.7149 (average: 0.7098, weighted according to Sr concentration; Dessert et al., 2001). While the isotope composition of runoff from this basalt province is atypical of large volcanic provinces, the Sr flux is likely more representative. However, owing to the radiogenic nature of river draining the Deccan traps, the flux of unradiogenic Sr ($^{87}Sr/^{86}Sr$ of 0.7035) from the Deccan traps is quite low, similar to that from Iceland.

These fluxes can be compared to Sr fluxes from small ocean islands (Rad et al., 2007), such as Martinique (1100 km^2, ~1.76 km^3 yr^{-1} surface runoff) and Guadeloupe (1179 km^2, ~3.54 km^3 yr^{-1} surface runoff) in the Lesser Antilles, and Réunion in the Indian Ocean (2512 km^2, ~6.28 km^3 yr^{-1} surface runoff). We compare the surface (river) runoff from these islands with river data from western South America, Iceland and the Deccan traps, but emphasize that the total Sr flux from these areas may be significantly higher if subterranean Sr fluxes are significant. While the lack of data for subterranean fluxes prevents us from quantifying such contributions for the drainage areas of western South America, Iceland or the Deccan traps, Rad et al. (2007) have quantified subsurface fluxes from small islands of the Lesser Antilles and Réunion. Contributions from surface runoff to the total Sr flux range from 20% (Martinique) to 30% (Réunion) and 60% (Guadeloupe). The unradiogenic Sr yield for these islands (see Fig. 3) could thus easily be higher by factors of 2 (Lesser Antilles) and 3 (Réunion) if the subterranean contributions are taken into account.

5.4. Global significance of unradiogenic Sr runoff from volcanically-dominated continental margins.

Runoff from western South America combines two important characteristics of runoff from Iceland and the Deccan Traps: unradiogenic Sr and high Sr yields. This drainage region thus yields abundant dissolved Sr that is isotopically more similar to high-temperature (HT) mid ocean ridge (MOR) vent fluids ($^{87}Sr/^{86}Sr$ of 0.70285-0.70465; Bach and Humphris, 1999) and volcanic islands (Louvat, 1997; Rad et al., 2007) than to average continental runoff ($^{87}Sr/^{86}Sr$ of 0.7119; Palmer and Edmond, 1989). We estimate the flux of unradiogenic ($^{87}Sr/^{86}Sr$ of 0.7035) Sr from this region using a model of two-component isotope mixing between an average upper crustal component ($^{87}Sr/^{86}Sr$ of 0.7119; Palmer and Edmond, 1989) and a HT MOR-vent component ($^{87}Sr/^{86}Sr$ of 0.7035; Palmer and Edmond, 1989). With this, the yield of unradiogenic riverine ($^{87}Sr/^{86}Sr$ of 0.7035) Sr from western South America is 377 moles Sr km^{-2} yr^{-1} (equivalent to a total flux of $4.6x10^{8}$ mole yr^{-1}), a factor of 2-3 higher than the yield of unradiogenic Sr from Iceland or the Deccan traps, and a factor of up to two lower that unradiogenic Sr yields from the Lesser Antilles and Réunion (gray symbols in Fig. 3). These yields do not include subterranean contributions that can be significant (e.g. Lesser Antilles, Réunion; Rad et al., 2007), but are not quantified for western South America, Iceland and the Deccan traps.

Estimates of magmatic heat dissipation ($6.3\text{-}12x10^{19}$ J yr^{-1}; Butterfield et al., 2001) for 0-1 Myr old MOR crust, average fluid temperature (350°C; Palmer and Edmond, 1989; 1624 J g^{-1}, Butterfield et al., 2001) and Sr concentration in such HT fluids (100 μM; Palmer and Edmond, 1989) allow us to compare the global flux of Sr from HT-vents ($3.9\text{-}7.4x10^{9}$ M yr^{-1}) with the flux of unradiogenic Sr from continental arcs. Per length of volcanically active arc (~5000 km for the

Andes), the yield of unradiogenic arc strontium ($9.2x10^4$ mole km^{-1} yr^{-1}) rivals the yield of Sr from HT fluids interacting with a young MOR segment of equivalent length ($7.8\text{-}14.8x10^4$ mole km^{-1} $yr\text{-}^{1}$; assuming a global MOR length of 50,000 km). Consequently, temporal variations in the flux of unradiogenic Sr from such unradiogenic continental arcs have the potential to contribute to the observed temporal variations in the seawater $^{87}Sr/^{86}Sr$ record.

Such temporal variations in runoff can be forced by the plate-tectonic movement of such areas into more humid climate zones. Increases in runoff can also be triggered by topographic uplift that leads to enhanced orographic rainfall and physical erosion (e.g. Ernst, 2004), and by higher temperatures that accelerate weathering reactions. Alternatively, a greater areal abundance of young active margins can lead to enhanced delivery of unradiogenic continental Sr to seawater. Such processes need to be considered as complementary mechanisms to variable submarine hydrothermal Sr emissions for modulating the flux of unradiogenic Sr to seawater (cf. Brass, 1976). However, models of the temporal evolution of unradiogenic Sr fluxes from volcanically-dominated active margins critically depend on reconstructing uplift histories of coastal mountain belts (e.g. Gregory-Wodzicki, 2000; Garzione et al., 2008) that induce orographic rainfall. Such reconstructions need to be focused on the initial uplift, as the first 1000-2000 meters uplift trigger most of the precipitation enhancement (Browning, 1980). Competing factors such as shifts in ocean currents that influence moisture transport to land also need to be taken into account. As the evolution of these factors has not been reconstructed with sufficient temporal resolution and spatial precision (i.e., typical uncertainties of paleoelevation estimates are on the order of 1000-1500 m; Gregory-Wodzicki, 2000; Carzione et al., 2008) for the drainage area of western South America, modeling the effects variable contributions of

293 unradiogenic Sr have had on the evolution of seawater $^{87}Sr/^{86}Sr$ would be highly speculative at
294 this point.

295

296 **6. Acknowledgments**

297 We thank Rhian Waller for help with the collection of some of the river samples, Tracy
298 Atwood for assistance in the lab, as well as Scot Birdwhistell and Jerzy Blusztajn for help with
299 the ICPMS analyses that were carried out in the NSF-supported WHOI ICPMS Facility (NSF
300 EAR 0651366). We also thank Jeff Seewald for giving us access to his ion chromatograph, and
301 Stan Hart for the use of his correction scheme for Kr interferences. We acknowledge financial
302 support from NSF grant EAR-0519387, from WHOI's Mary Sears Visitor Program, and thank
303 the German DAAD for travel support for KF. Comments by editor Bernard Bourdon and two
304 anonymous reviewers significantly improved this contribution.

305

306 **7. References**

307 Åberg, F., Wickman, F.E., 1987. Variations of $^{87}Sr/^{86}Sr$ in water from streams discharging into
308 the Bothnian Bay, Baltic Sea. Nordic Hydrology 18, 33-42.

309 Albarede, F., Michard, A., Minster, J.F., Michard, G., 1981. $^{87}Sr/^{86}Sr$ ratios in hydrothermal
310 waters and deposits from the East Pacific Rise at 21°N. Earth and Planetary Science Letters
311 55, 229-236.

312 Bach, W., Humphris, S.E., 1999. Relationship between the Sr and O isotope compositions of
313 hydrothermal fluids and the spreading and magma-supply rates at oceanic spreading centers.
314 Geology 27, 1067-1070.
315 Baumgartner A., Reichel, E., 1975. The World Water Balance. Elsevier, Amsterdam, 179 pp +
316 31 maps.
317 Brass, G.W., 1976. The variation in the marine $^{87}Sr/^{86}Sr$ ratio during Phanerozoic time:
318 interpretation using a flux model. Geochimica et Cosmochimica Acta 40, 721-730.
319 Browning, K.A., 1980. Structure, mechanism, and prediction of orographically enhanced rain in
320 Britain. Global Atmospheric Research Programme Publication Series 23, 85-114.
321 Butterfield, D.A., Nelson, B.K., Wheat, C.G., Mottl, M.J., Roe, K.K., 2001. Evidence for basaltic
322 Sr in midocean ridge-flank hydrothermal systems and implications for the global oceanic Sr
323 isotope balance. Geochimica et Cosmochimica Acta 65, 4141-4153
324 Cameron, E.M., Hattori, K., 1997. Strontium and neodymium isotope ratios in the Fraser River,
325 British Columbia: a riverine transect across the Cordilleran orogen. Chemical Geology 137,
326 243-253.
327 Carzione, C.N., Hoke, G.E., Libarkin, J.C., Withers, S., MacFadden, B., Eiler, J., Gosh, P.,
328 Mulch, A., 2008. Rise of the Andes. Science 320, 1304-1307.
329 Das, A., Krishnaswami, S., 2007. Elemental geochemistry of river sediments from the Deccan
330 Traps, India: Implications to sources of elements and their mobility during basalt-water
331 interaction. Chemical Geology 242, 232-254.
332 Dessert, C., Dupré, B., François, L.M., Schott, J., Gaillardet, J., Chakrapani, G.J., Bajpai, S.,
333 2001. Erosion of Deccan Traps determined by river geochemistry: impact on the global
334 climate and the $^{87}Sr/^{86}Sr$ ratio of seawater. Earth and Planetary Science Letters 188, 459-474.

335 Dirección General de Aguas, 1998. Water balance of Chile. Santiago de Chile.
336 Ernst, W.G., 2004. Regional crustal thickness and precipitation in young mountain chains.
337 Proceedings of the National Academy of Sciences of the United States of America 101 (42),
338 14,998-15,001.
339 Faure, G., Crocket, J. H., Hueley, P.M., 1967. Some aspects of the geochemistry of strontium
340 and calcium in the Hudson Bay and the Great Lakes. Geochimica et Cosmochimica Acta 31,
341 451-461.
342 Fisher, R.S., Stueber, A.M., 1976. Strontium isotopes in selected streams within the
343 Susquehanna river basin. Water Resources Research 12, 1061-1068.
344 Gannoun, A., Burton, K.W., Vigier, N., Gislason, S.R., Rogers, N., Mokadem, F., Sigfuson, B.,
345 2006. The influence of weathering process on riverine osmium isotopes in a basaltic terrain.
346 Earth and Planetary Science Letters 243, 732-748.
347 Gobierno de Chile, Ministerio de Obras Publicas, Dirección General de Aguas, Diciembre 2004.
348 Cuenca del Rio Rappel, Cade-Idepe Consultores en Ingenieria, 190 pp.
349 Goldstein, S.J., Jacobsen, S.B., 1987. The Nd and Sr isotope systematics of river-water dissolved
350 material: implications for the sources of Nd and Sr in seawater. Chemical Geology, 245-272.
351 Graham, S.T., Famiglietti, J.S., Maidment, D.R., 1999. Five-minute, ½°, and 1° data sets of
352 continental watersheds and river networks for use in regional and global hydrologic and
353 climate system modeling studies. Water Resources Research, 35(2), 583-587.
354 Graham, S.T., Famiglietti, J.S., Maidment, D.R., 2000. Five-minute, ½°, and 1° data sets of
355 continental watersheds and river networks for use in regional and global hydrologic and
356 climate system modeling studies: watershed and drainage network data evaluated at three
357 spatial resolutions with supporting documentation. Digital data on 5 minute, ½ degree and 1

degree resolution, geographic (lat/long) global grids. Boulder, CO: NOAA National Geophysical Data Center. Nine spatial layers with multiple attributes.

Gregory-Wodzicki, K., 2000. Uplift history of the Central and Northern Andes: A review. Geological Society of America Bulletin 112 (7), 1091-1105.

Habit, E., Belk, M., Victoriano, P., Jaque, E., 2007. Spatio-temporal distribution patterns and conservation of fish assemblages in a Chilean coastal river. Biodiversity Conservation 16, 3179-3191, doi: 10/1007/s10531-007-9171-9.

Hart, S.R., Ball, L., Jackson, M., 2004 (additions and revisions, Feb. 2005). Sr isotopes by laser ablation PIMMS: Application to cpx from Samoan peridotite xenoliths. WHOI Plasma Facility Open File Technical Report 11, (http://www.whoi.edu/science/GG/people/shart/open_file.htm).

Hickey, R.L., Frey, F.A., Gerlach, D.C., 1986. Multiple sources for basaltic arc rocks from the southern volcanic zone of the Andes (34°-41°S): Trace element and isotopic evidence for contributions from subducted oceanic crust, mantle, and continental crust. Journal of Geophysical Research 91 (B6), 5963-5983.

Louvat, P., 1997. Etude géochimique de l'érosion fluviale d'îles volcaniques à l'aide des bilans d'éléments majeurs et traces. Ph.D. thesis, Université Paris 7, 322 p.

McArthur, J.M., Howarth, R.J., 2004. Strontium isotope stratigraphy. In *A Geologic Time Scale 2004* (F.M. Gradstein, J.G. Ogg and A.G. Smith). Cambridge Univ. Press, Cambridge, UK, 96-105.

Muñoz, J.F., Fernandez, B., Vargas, E., Pastén, P., Gomez, D., Rengifo, P., Muñoz, J., Atenas, M., Jofré, J.C., 2007. Chilean water resources. In *The Geology of Chile* (T. Moreno and W. Gibbons, Eds.). Geological Society of London, Bath, 215-230.

New, M., Lister, D., Hulme, M., Makin, I., 2002. A high-resolution data set of surface climate over global land areas. Climate Research 21, 1-25.

Notsu, K., Lopez-Escobar, L., Onuma, N., 1987. Along-arc variation of Sr-isotope composition in volcanic rocks from the Southern Andes (33°S-55°S). Geochemical Journal 21, 307-313.

Palmer, M.R., Edmond, J.M., 1989. The strontium isotope budget of the modern ocean. Earth and Planetary Science Letters 92, 11-26.

Palmer, M.R., Edmond, J.M., 1992. Controls over the strontium isotope composition of river water. Geochimica et Cosmochimica Acta 56, 2099-2111.

Peucker-Ehrenbrink, B., Miller, M.W., 2007. Quantitative bedrock geology of the continents and large-scale drainage regions. Geochemistry, Geophysics, Geosystems 8 (5), Q06009, doi: 10.1029/2006GC001544.

Peucker-Ehrenbrink, B., 2009. Land2Sea database of river drainage basin sizes, annual water discharges, and suspended sediment fluxes. Geochemistry, Geophysics, Geosystems 10 (6), Q06014, doi:10.1029/2008GC002356.

Quiñones, R.A., Montes, R.M., 2001. Relationship between freshwater input to the coastal zone and the historical landings of the benthic/demersal fish *Eleginops maclovinus* in central-south Chile. Fisheries Oceanography 10 (4), 311-328.

Rad, S.D., Allègre, C.J., Louvat, P., 2007. Hidden erosion on volcanic islands. Earth and Planetary Science Letters 262, 109-124.

Rech, J.A., Quade, J., Hart, W.S., 2003. Isotopic evidence for the source of Ca and S in soil gypsum, anhydrite, and calcite in the Atacama Desert, Chile. Geochimica et Cosmochimica Acta 67, 575-586.

403 Stern, C.R., 2004. Active Andean volcanism: its geologic and tectonic setting. Revista
404 Geologica de Chile, 31 (2), 161-206.
405 Wadleigh, M.A., Veizer, J., Brooks, C., 1985. Strontium and its isotopes in Canadian rivers:
406 fluxes and global implications. Geochimica et Cosmochimica Acta 49, 1727-1736.
407
408 **Figure 1:** Map of South America, Chile (in gray) and sampling area (box). Inset shows
409 sampling locations (black circles) and outlines of Chilean river basins sampled in this study. The
410 northern Coastal basin includes the Andalien river basin. The southern Coastal basin includes
411 the Rio Cisne, the Rio Llonco and the Rio Huinay.
412
413 **Figure 2A:** Strontium (μM, logarithmic scale) versus calcium (mM, logarithmic scale)
414 concentrations in rivers draining Chile (filled circles), Iceland (small gray triangles; Gannoun et
415 al., 2006), the Indian Deccan Traps (open squares; Dessert et al., 2001), the Lesser Antilles (open
416 circles; Rad et al., 2007), and Reunion (large open triangles; Rad et al., 2007). The Chilean
417 sample CH049 (Rio Pichicolo) with very high Sr (see Fig. 2B) and Ca concentrations is not
418 shown.
419 **Figure 2B:** Strontium concentrations (μM, logarithmic scale) versus $^{87}Sr/^{86}Sr$ in Chilean (filled
420 circles), Lesser Antilles (open circles) and Reunion rivers (large open triangles). The average Sr
421 concentration (0.50 μM, 43 μg l^{-1}) and isotope composition ($^{87}Sr/^{86}Sr$=0.7057) of the Chilean
422 rivers, weighted according to water flux, is shown as a star.
423
424 **Figure 3:** Strontium yield (area-normalized Sr flux) versus specific surface runoff (area-
425 normalized water flux) from western South America (filled circle) the Deccan traps (squares),

Iceland (small gray triangle), Martinique and Guadeloupe (lesser Antilles, open circle), and Reunion (large triangle). The gray symbols represent the yield of unradiogenic Sr ($^{87}Sr/^{86}Sr$ of 0.7035) from these areas. In the case of Iceland the flux of unradiogenic Sr is assumed to be identical to the total Sr flux, because of the presumed unradiogenic nature of riverine Sr in Iceland (see text for details).

Table 1: Physical and chemical data for rivers in central and southern Chile.

Fiege et al. (CHEMGE4601, 2009) - Figure 1

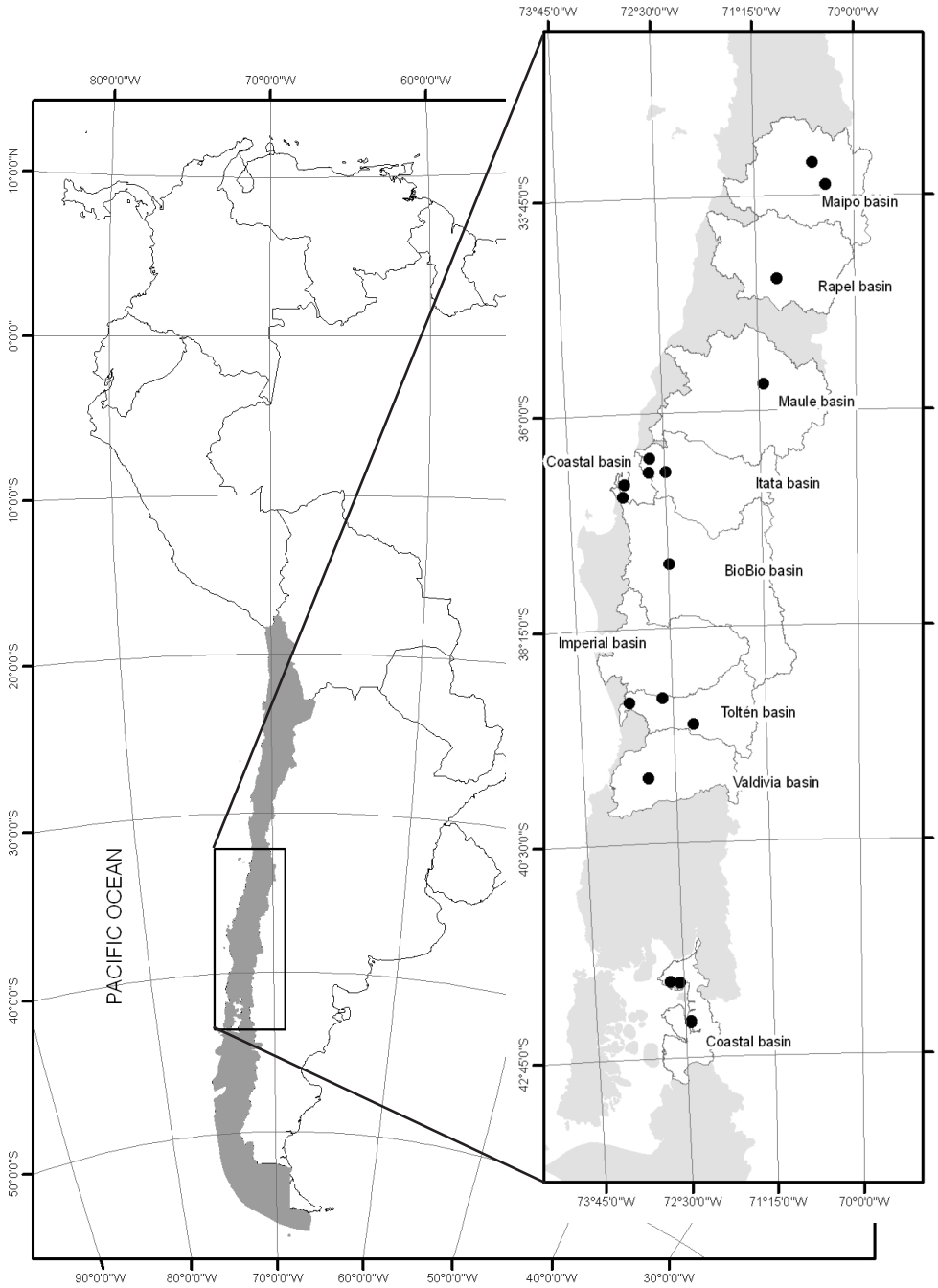

Fiege et al. (CHEMGE 4601, 2009) - Figure 2

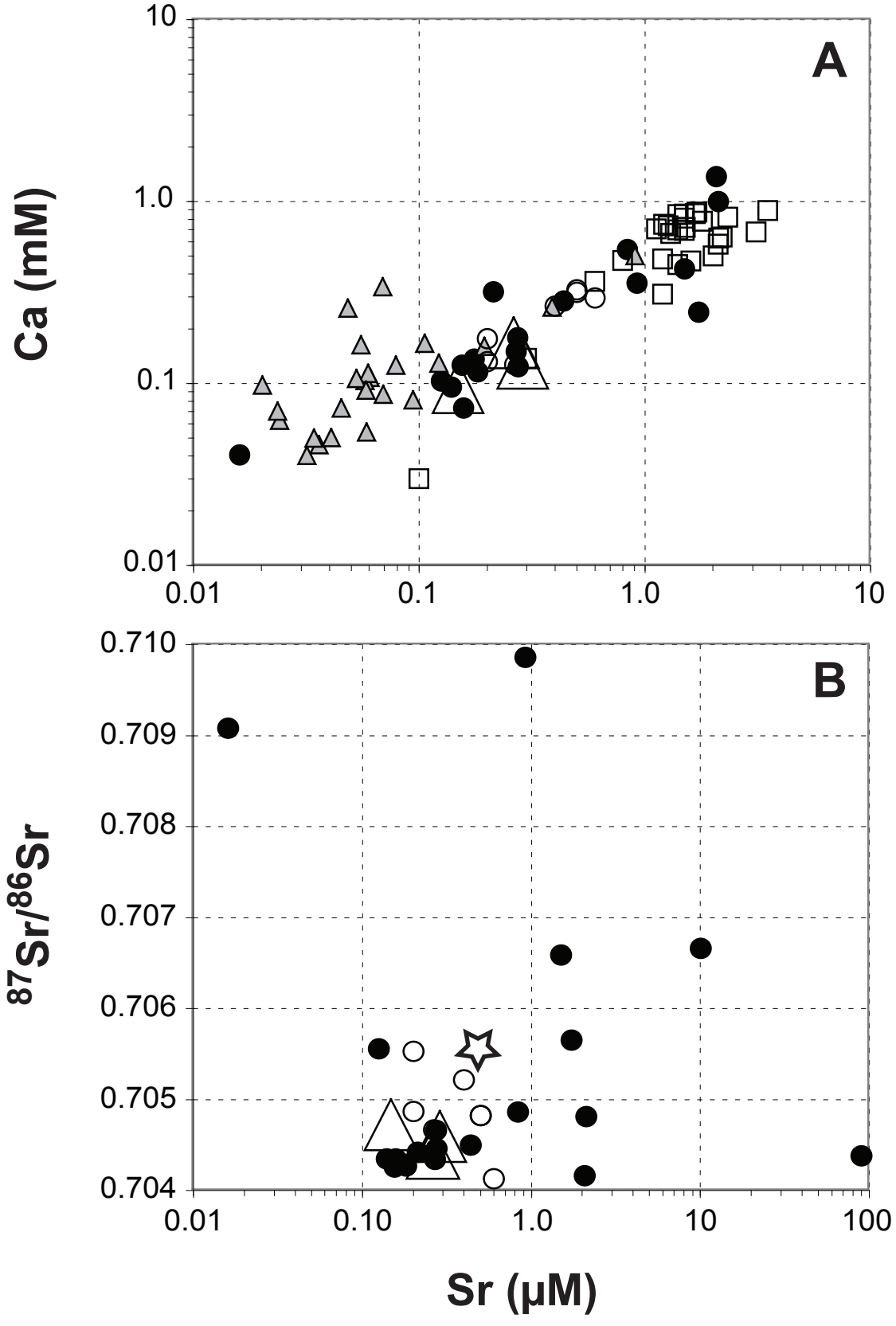

Fiege et al. (CHEMGE 4601, 2009) - Figure 3

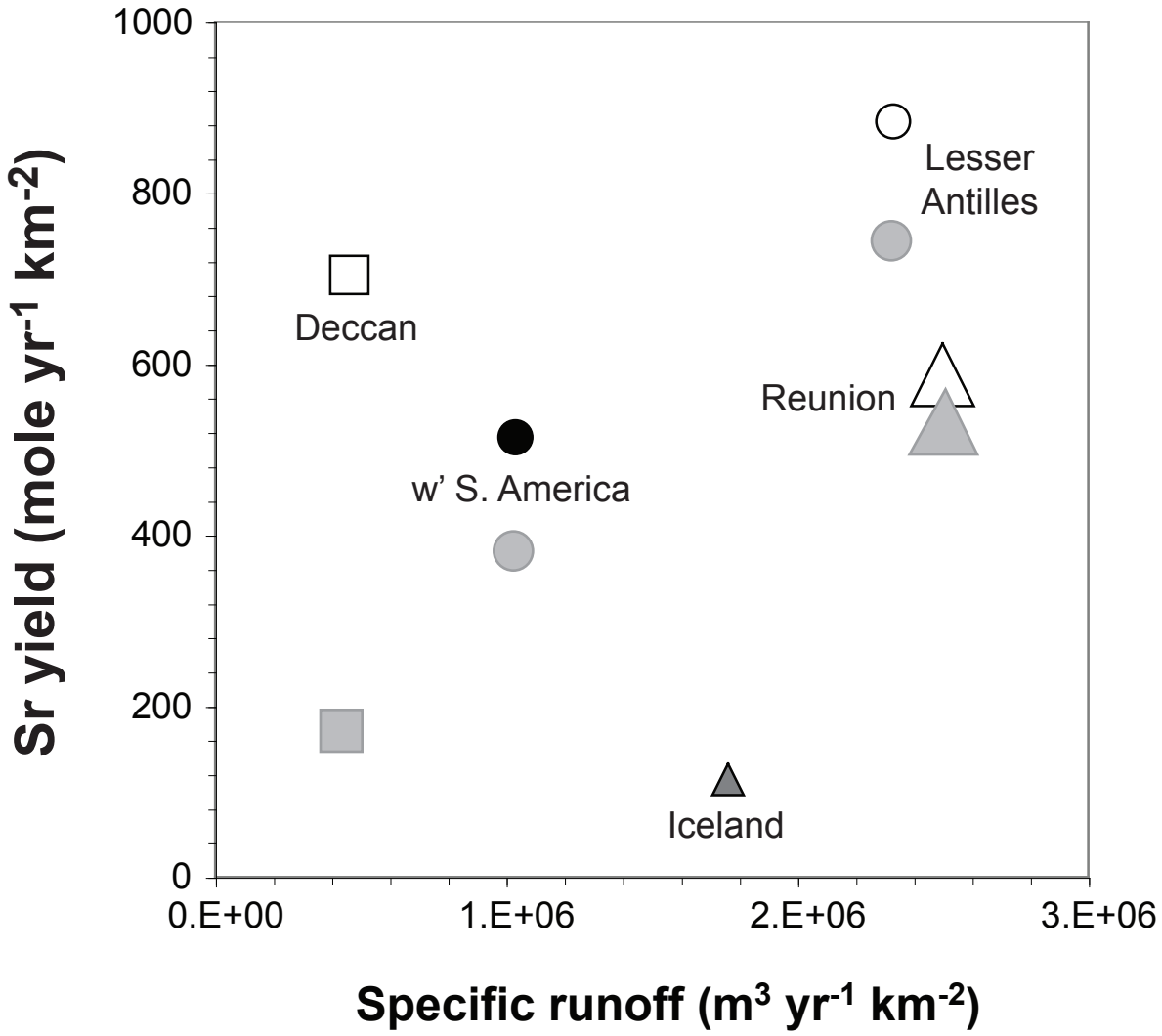

Table 1: Physical and chemical data for rivers in central and southern Chile

ID	River	Large River Basin	Total Drainage Basin	Runoff	Latitude	Longitude	Altitude	Date	Time	Temp.	pH	Conduct.	Cl^-	SO_4^{2-}	Na^+	Mg^{2+}	Ca^{2+}	K^+	Rb^+	Sr^{2+}	Ba^{2+}	$^{87}Sr/^{86}Sr$
units:			km^2	$km^3 yr^{-1}$	deg min S	deg min W	m	mm/dd/yr	24 h	°C		µS cm^{-1}	mM	µM	mM	mM	mM	mM	nM	µM	nM	
1 (CH001)	Mapocho				33°23.687'	70°31.279'	1227	01/28/07					0.15	1894	0.276	0.281	1.37	0.030	37.2	2.07	68.0	0.70416
3 (CH003)	Maipo	Maipo	**15,157**	**3.14**	33°37.729'	70°21.288'	940	01/29/07					2.49	3.30		0.387	3.69	0.070	73.9	**10.06**	85.6	**0.70666**
22 (Tg 1 Tinguiririca)	Tinguiririca	Rapel	**13,695**	**5.38**	34°36.750'	70°58.908'		09/16/06	10:30	9.5	8.6	128.6	0.16	366	0.328	0.110	0.545	0.026	38.6	**0.835**	25.3	**0.70486**
6 (CH013)	Maule	Maule	**20,865**	**17.96**	35°43.415'	71°10.578'	423	01/31/07					0.19	174	0.365	0.129	0.285	0.033	45.8	**0.436**	22.3	**0.70450**
7 (CH026)	Itata	Itata	11,385	11.39	36°27.997'	72°41.498'	17	02/02/07					0.33	3.5	0.905	0.472	0.428	0.046	3.03	1.50	0.13	0.70659
8 (IT 1 Itata 1)	Itata	Itata	11,385	11.39	36°37.453'	72°28.893'		06/28/06	15:20	11.2	7.3	73.2	0.053	29	0.189	0.094	0.124	0.022	24.3	0.275	19.7	0.70446
9 (IT 2 Itata 2)	Itata	Itata	**11,385**	**11.39**	36°37.453'	72°41.742'		06/29/06	17:00	10	6.8	79	0.055	34.2	0.177	0.080	0.150	0.026	21.7	**0.269**	22.5	**0.70434**
2 (CH02)	Andalien	Andalien	**~850**	**~0.48**	36°48.115'	73°58.004'		12/02/04	10:40				0.16	10.2	0.58	0.177	0.356	0.043	17	**0.921**	70.2	**0.70986**
4 (CH05)	BioBio	BioBio	**24,782**	**31.69**	36°52.128'	73°02.671'		12/02/04	9:00				0.088	50.7	0.238	0.099	0.179	0.025	22.7	**0.273**	18.2	**0.70466**
21 (BU 2 Bueno 2)	Bueno	BioBio	24,782	31.69	37°35.200'	72°28.508'		08/22/06					0.036	6.7	0.085	0.043	0.073	0.007	7.52	0.157	16.6	0.70435
11 (CH029)	Tolten	Tolten	8,040	18.4	38°58.633'	72°38.183'	226	02/03/07					0.049	28.1	0.202	0.075	0.126	0.025	22.5	0.155	24.5	0.70426
13 (TL 1 Tolten 1)	Tolten	Tolten	**8,040**	**18.4**	39°00.653'	73°04.907'		06/25/06	16:00	11	7.5	28.1	0.040	15.6	0.136	0.056	0.096	0.019	17.3	**0.139**	13.7	**0.70435**
12 (CH034)	Tolten	Tolten	8,040	18.4	39°16.46'	72°13.804'	223	02/04/07					0.035	19.3	0.159	0.066	0.116	0.023	22.4	0.182	12.5	0.70427
14 (CH038)	Calle Calle	Valdivia	**9,902**	**29.27**	39°48.595'	72°51.89'	14	02/04/07					0.038	16.2	0.118	0.046	0.103	0.016	16.4	**0.125**	21.0	**0.70556**
15 (CH048)	Cisne		**5,302**	**12.21**	41°57.492'	72°40.682'	34	02/06/07					0.045	12	0.125	0.083	0.136	0.016	11.3	**0.175**	22.7	**0.70429**
16 (CH049)	Pichicolo				41°58.495'	72°33.178'	73	02/06/07					2.78	606		0.034	0.320	0.021	39.7	0.213	8.7	0.70442
19 (CH058)	Llonco				42°22.434'	72°24.649'	0.3	02/06/07					0.033	12.2	0.042	0.008	0.041	0.006	4.6	0.016	18.9	0.70908
20 (CH059)	*Fundacion Huinay*				42°22.863'	72°24.929'	33	02/06/07					0.028	24.5	0.047	0.045	0.246	0.165	19.9	1.73	4.35	0.70565
W' South America			1,220,853	1,273																0.496		0.7057

Notes: Bold-faced numbers have been used for calculating regional averages.